# Irregular Breathing classification from Multiple Patient Datasets using Neural Networks

Suk Jin Lee [a], Yuichi Motai [a], Elisabeth Weiss [b], and Shumei S. Sun [c]

***Abstract*— Complicated breathing behaviors including uncertain and irregular patterns can affect the accuracy of predicting respiratory motion for precise radiation dose delivery [3-6, 25, 36]. So far investigations on irregular breathing patterns have been limited to respiratory monitoring of only extreme inspiration and expiration [37]. Using breathing traces acquired on a Cyberknife treatment facility, we retrospectively categorized breathing data into several classes based on the extracted feature metrics derived from breathing data of multiple patients. The novelty of this paper is that the classifier using neural networks can provide clinical merit for the statistical quantitative modeling of irregular breathing motion based on a regular ratio representing how many regular/irregular patterns exist within an observation period. We propose a new approach to detect irregular breathing patterns using neural networks, where the reconstruction error can be used to build the distribution model for each breathing class. The proposed irregular breathing classification used a regular ratio to decide whether or not the current breathing patterns were regular. The sensitivity, specificity, and receiver operating characteristic (ROC) curve of the proposed irregular breathing pattern detector was analyzed. The experimental results of 448 patients' breathing patterns validated the proposed irregular breathing classifier.**

***Index Terms*— Abnormal detection, neural networks, breathing classification, irregular respiration, receiver operating characteristic.**

## I. Introduction

RAPID developments in image-guided radiation therapy offer the potential of precise radiation dose delivery to most patients with early or advanced lung tumors [1-6]. While early stage lung tumors are treated with stereotactic methods, locally advanced lung tumors are treated with highly conformal radiotherapy, such as intensity modulated radiotherapy (IMRT) [2]. Both techniques are usually planned based on four-dimensional computed tomography [1]. Thus, the prediction of individual breathing cycle irregularities is likely to become very demanding since tight safety margins will be used. Safety margins are defined based on the initial planning scan that also analyzes the average extent of breathing motion, but not the individual breathing cycle. In the presence of larger respiratory excursions, treatment can be triggered by respiration motion in such a way that radiation beams are only on when respiration is within predefined amplitude or phase [39]. Since margins are smaller with more conformal therapies, breathing irregularities might become more important unless there is a system in place that can stop the beam in the presence of breathing irregularities. Real-time tumor-tracking, where the prediction of irregularities really becomes relevant [25], has yet to be clinically established.

The proposed methodology for irregular breathing classification can impact the dose calculation for patient treatments [12-13]. The highly irregularly breathing patient may be expected to have a much bigger internal target volume (ITV) than a regular one, where ITV contains the macroscopic cancer and an internal margin to take into account the variations due to organ motions [12]. Thus, the detection of irregular breathing motion before and during the external beam radiotherapy is desired for minimizing the safety margin [13]. Only a few clinical studies, however, have shown a deteriorated outcome with increased irregularity of breathing patterns [1, 13, 25], probably due to the lack of technical development in this topic. Other reasons confounding the clinical effect of irregular motion such as variations in target volumes or positioning uncertainties also influence the classification outcomes [12-14, 25]. The newly proposed statistical classification may provide clinically significant contributions to minimize the safety margin during external beam radiotherapy based on the breathing regularity classification for the individual patient. An expected usage of the irregularity detection is to adapt the margin value, *i.e.*, the patients classified with regular breathing patterns would be treated with tight margins to minimize the target volume. For patients classified with irregular breathing patterns safety margins may need to be adjusted based on the irregularity to cope with baseline shifts or highly fluctuating amplitudes that are not covered by standard safety margins [12-13].

There exists a wide range of diverse respiration patterns in human subjects [8-14]. However, the decision boundary to distinguish the irregular patterns from diverse respirations is not clear yet [14, 37]. For example, some studies defined only two (characteristic and uncharacteristic [13]) or three (small, middle, and large [12]) types of irregular breathing motions based on the breathing amplitude to access the target dosimetry [12-13]. Our purpose is to classify irregular patterns, given symptoms that fit into neither the regular pattern nor the regular compression pattern categorizations [23]. Respiratory patterns can be classified as normal or abnormal patterns [37]. The key point of the classification as normal or abnormal breathing patterns is how to extract the dominant feature from the original breathing datasets [15-16, 32-35, 40]. For example, Lu *et al*. calculated a moving average curve using a fast Fourier transform to detect respiration amplitudes [37]. Some studies showed that the flow volume curve with neural networks can be used for the classification of normal and abnormal respiratory patterns [9-10]. However, spirometry data are not commonly used for abnormal breathing detection during image-guided

[a] Department of Electrical and Computer Engineering, Virginia Commonwealth University, Richmond, VA 23284. Email: leesj9@mymail.vcu.edu, ymotai@vcu.edu.
[b] Department of Radiation Oncology, Virginia Commonwealth University, Richmond, VA 23298. Email: eweiss@mcvh-vcu.edu.
[c] Department of Biostatistics, Virginia Commonwealth University, Richmond, VA 23298. Email: ssun@vcu.edu.

radiation therapy [9].

To detect irregular breathing, we present a method that retrospectively classifies breathing patterns using multiple patients-breathing data originating from a Cyberknife treatment facility [17]. There is no implicit assumption made for the future breathing patterns at the time of treatment. The multiple patients-breathing data contain various breathing patterns. For the analysis of breathing patterns, we extracted breathing features, *e.g.* vector-oriented feature [34-35], amplitude of breathing cycle [36-37] and breathing frequency [14], *etc*., from the original dataset, and then classified the whole breathing data into classes based on the extracted breathing features. To detect irregular breathing, we introduce the reconstruction error using neural networks as the adaptive training value for anomaly patterns in a class.

The contribution of this paper is threefold: First, we propose a new approach to detect abnormal breathing patterns with multiple patients-breathing data that better reflect tumor motion in a way needed for radiotherapy than the spirometry. Second, the proposed new method achieves the best irregular classification performance by adopting Expectation-Maximization (EM) based on the Gaussian Mixture model with the usable feature combination from the given feature extraction metrics. Third, we can provide clinical merits with prediction for irregular breathing patterns, such as to validate classification accuracy between regular and irregular breathing patterns from ROC curve analysis, and to extract a reliable measurement for the degree of irregularity. This paper is organized as follows. In Section II, the theoretical background for the irregular breathing detection is discussed briefly. In Section III, the proposed irregular breathing detection algorithm is described in detail with the feature extraction method. The experimental results are presented in Section IV. A summary of the performance of the proposed method and conclusion are presented in Section V.

## II. Background

Modeling and prediction of respiratory motion are of great interest in a variety of applications of medicine [7, 18-21]. Variations of respiratory motions can be represented with statistical means of the motion [19] which can be modeled with finite mixture models for modeling complex probability distribution functions [22]. This paper uses the expectation-maximization (EM) algorithm for learning the parameters of the mixture model [26, 41]. In addition, neural networks are widely used for breathing prediction and for classifying various applications because of the dynamic temporal behavior with their synaptic weights [4, 23-25, 38]. Therefore, we use neural networks to detect irregular breathing patterns from feature vectors in given samples.

### *A. Expectation-Maximization (EM) based on Gaussian Mixture model*

A Gaussian mixture model is a model-based approach that deals with clustering problems in attempting to optimize the fit between the data and the model. The joint probability density of the Gaussian mixture model can be the weighted sum of $m > 1$ components $\phi(x|\ \mu_m, \Sigma_m)$. Here $\phi$ is a general multivariate Gaussian density function, expressed as follows [26]:

$$\phi(x \mid \mu_m, \Sigma_m) = \frac{\exp\left[-\frac{1}{2}(x-\mu_m)^T \sum_m^{-1}(x-\mu_m)\right]}{(2\pi)^{d/2}\left|\Sigma_m\right|^{1/2}}, \quad (1)$$

where $x$ is the $d$-dimensional data vector, and $\mu_m$ and $\Sigma_m$ are the mean vector and the covariance matrix of the $m^{th}$ component, respectively. A variety of approaches to the problem of mixture decomposition have been proposed, many of which focus on maximum likelihood methods such as the EM algorithm [41].

An EM algorithm is a method for finding maximum likelihood estimates of parameters in a statistical model. EM alternates between an expectation step, which computes the expectation of the log-likelihood using the current variable estimate, and a maximization step, which computes parameters maximizing the expected log-likelihood collected from the E-step. These estimated parameters are used to select the distribution of variable in the next E-step [22]. The EM was applied due to the unsupervised nature of unlabeled datasets.

### *B. Neural Network (NN)*

A neural network is a mathematical model or computational model that is inspired by the functional aspects of biological neural networks [27]. A simple NN consists of an input layer, a hidden layer, and an output layer, interconnected by modifiable weights, which are represented by links between the layers. Our interest is to extend the use of such networks to pattern recognition, where network input vector ($x_i$) denotes elements of extracted breathing features from the breathing dataset and intermediate results generated by network outputs will be used for classification with discriminant criteria based on clustered degree. Each input vector $x_i$ is given to neurons of the input layer, and the output of each input element is made equal to the corresponding element of the vector. The weighted sum of its inputs is computed by each hidden neuron $j$ to produce its net activation (simply denoted as $net_j$). Each hidden neuron $j$ gives a nonlinear function output of its net activation $\Phi(\cdot)$, *i.e.*, $\Phi(net_j) = \Phi(\Sigma^N_{i=1} x_i w_{ji} + w_{j0})$ in (2). The process of output neuron ($k$) is the same as the hidden neuron. Each output neuron $k$ calculates the weighted sum of its net activation based on hidden neuron outputs $\Phi(net_j)$ as follows [28]:

$$net_k = \sum_{j=1}^{H} w_{kj} \Phi\left(\sum_{i=1}^{N} x_i w_{ji} + w_{j0}\right) + w_{k0}, \quad (2)$$

where $N$ and $H$ denote neuron numbers of the input layer and hidden layer. The subscripts $i$, $j$ and $k$ indicate elements of the input, hidden, and output layers, respectively. Here, the subscript 0 represents the bias weight with the unit input vector ($x_0$=1). We denote the weight vectors $w_{ji}$ as the input-to-hidden layer weights at the hidden neuron $j$ and $w_{kj}$ as the hidden-to-output layer weights at the output neuron $k$. Each output neuron $k$ calculates the nonlinear function output of its *net* activation $\Phi(net_k)$ to give a unit for the pattern recognition.

## III. Proposed Irregular Breathing Classifier

As shown in Fig. 1, we first extract the breathing feature vector from the given patient datasets in Section A. The extracted feature vector can be classified with the respiratory pattern based on EM in Section B. Here, we assume that each

class describes a regular pattern. In Section C, we will calculate a reconstruction error for each class using a neural network. Finally, in Section D, we show how to detect the irregular breathing pattern based on the reconstruction error.

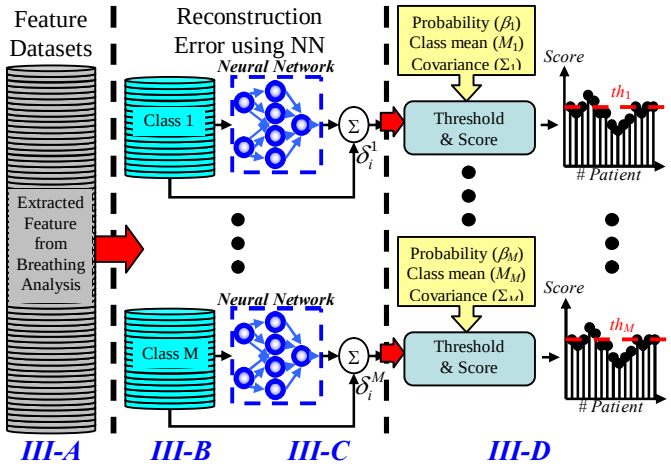


Fig. 1. Irregular Breathing Pattern Detection with the proposed algorithm.

The proposed process flow is to first find out the feasible feature vector for the efficient classification of breathing patterns based on the discriminant criterion [28] while assuming that each class describes a regular pattern, and then to select the classes of the breathing patterns using the feature vector based on the EM algorithm.

### *A. Feature Extraction from Breathing Analysis*

Feature extraction is a preprocessing step for classification by extracting the most relevant data information from the raw data [34]. In this study, we extract the breathing feature from patient breathing datasets for the classification of breathing patterns.

TABLE I
FEATURE EXTRACTION METRICS INCLUDING THE FORMULA AND NOTATION

| Name | Formula |
|---|---|
| AMV (Autocorrelation MAX value) | $\max[R_{xx}]$, $R_{xx}(\tau)=\frac{1}{2T}\int_{-T}^{T}x(t)x(t+\tau)dt$ ($T$ : period of observation) |
| ADT (Autocorrelation delay time) | $\arg\max_{\tau} R_{xx}(\tau)-\arg\min_{\tau} R_{xx}(\tau)$ |
| ACC (Acceleration variance) | $\mathrm{var}(\Delta x/\Delta t^2)$ ($x$ : observed breathing data) |
| VEL (Velocity variance) | $\mathrm{var}(\Delta x/\Delta t)$ |
| BRF (Breath Frequency) | $mean(1/BC_i)$ $BC_i$ : $i^{th}$ breathing cycle range |
| FTP (Max Power of Fourier transform) | $\max X$, $X(k)=\sum_{n=1}^{N}x(n)e^{-j2\pi(k-1)\left(\frac{n-1}{N}\right)}$ ($N$ : vectors of length $N$, $1\le k\le N$) |
| PCA (Principal Component Analysis Coefficient) | Y = $PrinComp$(X) ($PrinComp(\cdot)$:PCA function, X: data matrix ($N\times M$, $M$=3), Y: coefficient matrix ($M\times M$)) |
| MLR (Multiple Linear Regression Coefficient) | $\left(Z^TZ\right)^{-1}Z^Ty$ (Z: predictor, $y$: observed response) |
| STD (Standard deviation of time series data) | $s_N=\sqrt{\frac{1}{N}\sum_{i=1}^{N}(x_i-\bar{x})^2}$ |
| MLE (Maximum Likelihood Estimates) | $\hat{\theta}_{mle}=\arg\max_{\theta\in\Theta}\hat{F}(\theta\mid x_1,...,x_N)$, $\hat{F}=\frac{1}{N}\sum_{i=1}^{N}\ln f(x_i\mid\theta)$ |
| | $f(\cdot\mid\theta)$: Normal Distribution |

The typical vector-oriented feature extraction including principal component analysis (PCA) and multiple linear regressions (MLR) have been widely used [34-35]. Murphy *et al*. showed that autocorrelation coefficient and delay time can represent breathing signal features [25]. Each breathing signal may be sinusoidal variables [36] so that each breathing pattern can have quantitative diversity of acceleration, velocity, and standard deviation based on breathing signal amplitudes [37]. Breathing frequency also represents breathing features [14].

Table I shows the feature extraction metrics for the breathing pattern classification. We create Table I based on previous entities for breathing features, so that the table can be variable. The feature extraction metrics can be derived from multiple patient datasets with the corresponding formula. To establish feature metrics for breathing pattern classification, we define the candidate feature combination vector ( $\bar{x}$ ) from the combination of feature extraction metrics in Table I. We defined 10 feature extraction metrics in Table I. The objective of this section is to find out the estimated feature metrics ( $\check{\bar{x}}$ ) from the candidate feature combination vector ( $\bar{x}$ ) using discriminant criterion based on clustered degree. We can define the candidate feature combination vector as $\bar{x}$ =($x_1$,..., $x_z$), where variable $z$ is the element number of feature combination vector, and each element corresponds to each of the feature extraction metrics depicted in Table I. For example, let us define the number of feature combination vectors as three ($z$=3), where the feature combination vector can be $\bar{x}$ =(BRF, PCA, STD) with three out of 10 feature metrics. The total number of feature combination vectors using feature extraction metrics can be the summation of the combination function $C(10,z)$ as regards to $z$ objects ($z$=2,..., 10), where the combination function $C(10, z)$ is the number of ways of choosing $z$ objects from ten feature metrics. For the intermediate step, we may select which features to use for breathing pattern classification with the feature combination vectors, *i.e.*, the estimated feature metrics ( $\check{\bar{x}}$ ). For the efficient and accurate classification of breathing patterns, selection of relevant features is important [40]. In this study, the discriminant criterion based on clustered degree can be used to select the estimated feature metrics, *i.e.*, objective function $J(\cdot)$ using within-class scatter ($S_W$) and between-class scatter ($S_B$) [28-29]. Here we define the $S_W$ as follows:

$$S_W=\frac{1}{z}\sum_{i=1}^{G}S_i,\quad S_i=\sum_{j=1}^{n_i}(\bar{x}_{ij}-u_i)^2,\quad u_i=\frac{1}{n_i}\sum_{j=1}^{n_i}\bar{x}_{ij}, \tag{3}$$

where $z$ is the element number of a feature combination vector in $S_W$, $G$ is the total number of class in the given datasets, $S_i$ is the sum of squares of vectors within *i-th* class, and $n_i$ is the data number of the feature combination vector in the *i-th* class. We define the $S_B$ as follows:

$$S_B=\sum_{i=1}^{G}n_i\times(u_i-u)^2,\quad u=\frac{1}{n}\sum_{i=1}^{n}\bar{x}_i, \tag{4}$$

where $n$ is the total data number of the feature combination vector. The objective function $J$ to select the optimal feature combination vector can be written as follows:

$$J(\vec{x}) = \arg\min_{\vec{x}} \left( \frac{S_W}{S_B} \right), \quad (5)$$

where $\vec{x}$ can be the estimated feature vector for the rest of the modules for breathing patterns classification.

As shown in Section IV.A, three channel breathing datasets with a sampling frequency of 26 Hz are used to evaluate the performance of the proposed irregular breathing classifier. Here, each channel makes a record continuously in three dimensions for 448 patient datasets. The breathing recording time for each patient is distributed from 18 minutes to 2.7 hours, with 80 minutes as the average time at the Georgetown University CyberKnife treatment facility.

### *B. Clustering of Respiratory Patterns based on EM*

This section is aimed at finding the optimal number of clustering of respiratory patterns in the given datasets. We assume that the total 448 patientsô breathing patterns can be categorized into several classes (M), where each class ($m$) is optimized with the finite mixture model. We increase the M (from 2 to 8 in Section IV.C) components to optimize the Gaussian mixture model using the EM algorithm.

After extracting the estimated feature vector ($\vec{x}$) for the breathing feature, we can model the joint probability density that consists of the mixture of Gaussians $\phi(\vec{x}|\mu_m, \Sigma_m)$ for the breathing feature as follows [22, 26]:

$$p(\vec{x}, \Theta) = \sum_{m=1}^{M} \alpha_m \phi(\vec{x}|\, \mu_m, \Sigma_m), \quad \alpha_m \geq 0, \quad \sum_{m=1}^{M} \alpha_m = 1, \quad (6)$$

where $\vec{x}$ is the $d$-dimensional feature vector, $\alpha_m$ is the prior probability, $\mu_m$ is the mean vector, $\Sigma_m$ is the covariance matrix of the $m^{th}$ component data, and the parameter $\Theta \equiv \{\alpha_m, \mu_m, \Sigma_m\}_{m=1}^{M}$ is a set of finite mixture model parameter vectors. For the solution of the joint distribution $p(\vec{x}, \Theta)$, we assume that the training feature vector sets $\vec{x}_k$ are independent and identically distributed, and our purpose of this section is to estimate the parameters $\{\alpha_m, \mu_m, \Sigma_m\}$of the $M$ components that maximize the log-likelihood function as follows [26, 41]:

$$L(M) = \sum_{k=1}^{K} \log p(\vec{x}_k, \Theta), \quad (7)$$

where $M$ and $K$ are the total cluster number and the total number of patient datasets, respectively. Given an initial estimation $\{\alpha_0, \mu_0, \Sigma_0\}$, E-step in the EM algorithm calculates the posterior probability $p(m|\vec{x}_k)$ as follows:

$$p(m \mid \vec{x}_k) = \alpha_m^{(t)} \phi(\vec{x}_k \mid \mu_m^{(t)}, \Sigma_m^{(t)}) \Big/ \sum_{m=1}^{M} \alpha_m^{(t)} \phi(\vec{x}_k \mid \mu_m^{(t)}, \Sigma_m^{(t)}), \quad (8)$$

and then M-step is as follows:

$$\begin{aligned} \alpha_m^{(t+1)} &= \frac{1}{K} \sum_{k=1}^{K} p(m \mid \vec{x}_k) \\ \mu_m^{(t+1)} &= \frac{\sum_{k=1}^{K} p(m \mid \vec{x}_k) \vec{x}_k}{\sum_{k=1}^{K} p(m \mid \vec{x}_k)} = \frac{1}{\alpha_m K} \sum_{k=1}^{K} p(m \mid \vec{x}_k) \vec{x}_k \\ \Sigma_m^{(t+1)} &= \frac{1}{\alpha_m K} \sum_{k=1}^{K} p(m \mid \vec{x}_k) \left[ (\vec{x}_k - \mu_k^{(t+1)})(\vec{x}_k - \mu_k^{(t+1)})^T \right] \end{aligned} \quad . \quad (9)$$

With (8) in the E-step, we can estimate the $t^{th}$ posterior probability $p(m|\vec{x}_k)$. Based on this estimate result the prior probability ($\alpha_m$), the mean ($\mu_m$) and the covariance ($\Sigma_m$) in the $(t+1)^{th}$ iteration can be calculated using (9) in the M-step. Based on clustering of respiratory patterns, we can make a class for each breathing feature with the corresponding feature vector ($\vec{x}^m$) of class $m$. With the classified feature combination vector ($\vec{x}^m$), we can get the reconstruction error for the preliminary step to detect the irregular breathing pattern.

For the quantitative analysis of the cluster models, we use two criteria for model selection, *i.e.*, Akaike information criterion (AIC) and Bayesian information criterion (BIC), among a class of parametric models with different cluster numbers [31]. Both criteria measure the relative goodness of fit of a statistical model. In general, the AIC and BIC are defined as follows: $AIC = 2k - 2\ln(L)$, $BIC = -2\cdot\ln L + k\ln(n)$, where $n$ is the number of patient datasets, $k$ is the number of parameters to be estimated, and $L$ is the maximized log-likelihood function for the estimated model that can be derived from (7).

### *C. Reconstruction Error for Each Cluster using NN*

Using the classification based on EM, we can get M classes of respiratory patterns, as shown in Fig. 1. With the classified feature vectors ($\vec{x}^m$), we can reconstruct the corresponding feature vectors ($o^m$) with the neural networks in Fig. 2 and get the following output value,

$$o^m = \Phi\left( \sum_{j=1}^{H} w_{kj} \Phi\left( \sum_{i=1}^{N} \vec{x}_i^m w_{ji} + w_{j0} \right) + w_{k0} \right), \quad (10)$$

where $\Phi$ is the nonlinear activation function, and $N$ and $H$ denote the total neuron number of input and hidden layers, respectively. The neural weights ($w$) are determined by training samples of multiple patient datasets for each class M. Then, the neural networks using a multilayer perceptron for each class in Fig. 2 calculate the reconstruction error ($\delta^m$) for each feature vector $\vec{x}_i$ as follows [23]:

$$\delta_i^m = \frac{1}{F} \sum_{f=1}^{F} \left( \vec{x}_{if}^m - o_{if}^m \right)^2, \quad (11)$$

where $i$ is the number of patient datasets in a class $m$, and $f$ is the number of features. After calculating the reconstruction error ($\delta^m$) for each feature vector in Fig. 2, $\delta^m$ can be used to detect the irregular breathing pattern in the next section.

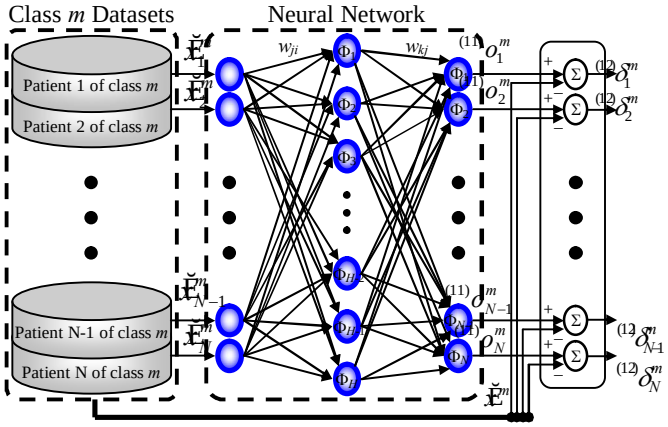


Fig. 2. Reconstruction Error to detect the irregular pattern using NN.

*D. Detection of Irregularity based on Reconstruction Error*

For the irregular breathing detection, we introduce the reconstruction error ($\delta^m$), which can be used as the adaptive training value for anomaly pattern in a class $m$. With the reconstruction error ($\delta^m$), we can construct the distribution model for each cluster $m$. That means the patient data with small reconstruction error can have a much higher probability of becoming regular than the patient data with many reconstruction errors in our approach. For class $m$, the probability ($\beta_m$), class means ($\nu_m$), and covariance $\Sigma_m$ can be determined as follows:

$$\beta_m = \frac{1}{K}\sum_{i=1}^{K} I(m \mid \vec{\mathbf{x}}_i), \tag{12}$$

$$\nu_m = \frac{\sum_{i=1}^{K} I(m \mid \vec{\mathbf{x}}_i)\delta_i^m}{\sum_{i=1}^{K} I(m \mid \vec{\mathbf{x}}_i)} = \frac{1}{\beta_m K}\sum_{i=1}^{K} I(m \mid \vec{\mathbf{x}}_i)\delta_i^m, \tag{13}$$

$$\Sigma_m = \frac{1}{\beta_m K}\sum_{i=1}^{K} I(m \mid \vec{\mathbf{x}}_i)\left[(\vec{\mathbf{x}}_i - M_m)(\vec{\mathbf{x}}_i - M_m)^T\right], \tag{14}$$

where $I(m|\vec{\mathbf{x}}_i)=1$ if $\vec{\mathbf{x}}_i$ is classified into class $m$; otherwise $I(m|\vec{\mathbf{x}}_i)=0$, $M_m$ is the mean value of the classified feature vectors ($\vec{\mathbf{x}}^m$) in class $m$, and $K$ is the total number of the patient datasets. To decide the reference value to detect the irregular breathing pattern, we combine the class means (13) and the covariance (14) with the probability (12) for each class as follows:

$$\bar{\nu} = \frac{1}{M}\sum_{m=1}^{M}\beta_m \nu_m, \quad \bar{\Sigma} = \frac{1}{M}\sum_{m=1}^{M}\beta_m \Sigma_m . \tag{15}$$

With (15), we can make the threshold value ($\xi_m$) to detect the irregular breathing pattern in (16), as follows:

$$\xi_m = \frac{(\nu_m - \bar{\nu})\sqrt{\bar{\Sigma}}}{L_m}, \tag{16}$$

where $L_m$ is the total number of breathing data in class $m$. For each patient $i$ in class $m$, we define $P_m$ as a subset of the patient whose score ($\delta^m{}_i$) is within the threshold value ($\xi_m$) in class $m$ and $1-P_m$ as a subset of the patient whose score ($\delta^m{}_i$) is greater than the threshold value ($\xi_m$) in class $m$, as shown in Fig. 3.

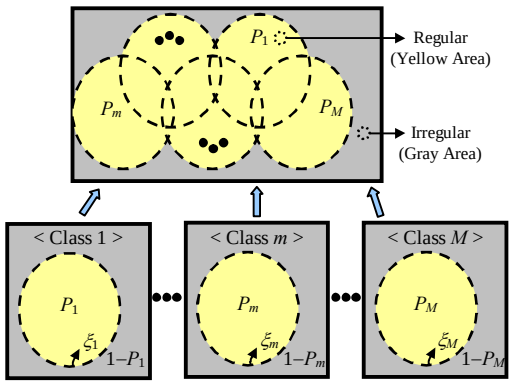


Fig. 3. Detection of regular/irregular patterns using the threshold value ($\xi_m$)

The digit ñ1ò represents the entire patient set for class $m$ in Fig. 3. With Fig. 3 we can detect the irregular breathing patterns in the given class $m$ with the threshold value ($\xi_m$). Accordingly, all the samples within the threshold value highlighted with yellow in Fig. 3 can be the regular respiratory patterns, whereas the other samples highlighted with gray in Fig. 3 can become the irregular respiratory patterns.

Fig. 3 shows that the threshold value ($\xi_m$) depicted by dotted lines can divide the regular respiratory patterns ($P_m$) from the irregular respiratory patterns ($1-P_m$) for each class $m$. As shown in Fig. 3, we can summarize the process of the regular/irregular breathing detection, and denote the regular respiratory patterns highlighted with yellow as $\cup^M_{m=1}(P_m)$ and the irregular respiratory patterns highlighted with gray as $\cap^M_{m=1}(1-P_m)$. We will use these notations for the predicted regular/irregular patterns in the following section.

*E. Evaluation Method for Irregular Classifier*

We apply standard sensitivity and specificity criteria as statistical measures of the performance of a binary classification test for irregularity detection. The classifier result may be positive, indicating an irregular breathing pattern as the presence of an anomaly. On the other hand, the classifier result may be negative, indicating a regular breathing pattern as the absence of the anomaly. Sensitivity is defined as the probability that the classifier result indicates a respiratory pattern has the anomaly when in fact they do have the anomaly. Specificity is defined as the probability that the classifier result indicates a respiratory pattern does not have the anomaly when in fact they are anomaly-free [30]. For the sensitivity and specificity, we can use Fig. 3 as the hypothesized class, *i.e.*, the predicted regular and irregular patterns, as follows:

$$FN + TN = \bigcup_{m=1}^{M} P_m, \quad TP + FP = \bigcap_{m=1}^{M}(1 - P_m) \cdot \tag{17}$$

The proposed classifier should have high sensitivity and high specificity. The given patient data show that the breathing data can be mixed up with the regular and irregular breathing patterns in Fig. 4. There are as yet no gold standard ways of labeling regular or irregular breathing signals. Lu *et al*. showed, in a clinical way, that the moving average value can be used to detect irregular patterns where inspiration or expiration was considered irregular if its amplitude was smaller than 20% of the average amplitude [37]. In this study, for the evaluation of the proposed classifier of abnormality, we define all the breathing patterns that are smaller than half the size of the average breathing amplitude as irregular patterns, shown with dotted lines in Fig. 4. During the period of observation ($T$), we noticed some irregular breathing patterns. Let us define $BC_i$ as the breathing cycle range for the patient $i$ as shown in Table I and $\psi_i$ as the number of irregular breathing pattern regions between a maximum (peak) and a minimum (valley).

For the patient $i$, we define the true positive/negative ranges ($R_i^{TP}/R_i^{TN}$) and the regular ratio ($\gamma_i$) as follows:

$$R_i^{TP} = \frac{BC_i}{2}\sum_j \psi_{ij}, \quad R_i^{TN} = T_i - \frac{BC_i}{2}\cdot\sum_j \psi_{ij}, \quad \gamma_i = \frac{R_i^{TN}}{T_i}, \tag{18}$$

where the ratio ($\gamma_i$) is variable from 0 to 1. For the semi-supervised learning of the TP and TN in the given patient datasets, we used the ratio ($\gamma_i$) of the true negative range ($R_i^{TN}$) to the period of observation ($T_i$) in (18). Let us denote $\Psi_{th}$ as the regular threshold to decide whether the patient dataset is regular or not. For patient $i$, we would like to decide a TP or TN based on values with the ratio ($\gamma_i$) and the regular threshold ($\Psi_{th}$), *i.e.*, if the ratio ($\gamma_i$) of patient $i$ is greater than the regular threshold ($\Psi_{th}$), the patient is true negative, otherwise ($\gamma_i \le \Psi_{th}$) true positive. We should notice also that the regular threshold

can be variable from 0 to 1. Accordingly, we will show the performance of sensitivity and specificity with respect to the variable regular threshold in Section IV.E.

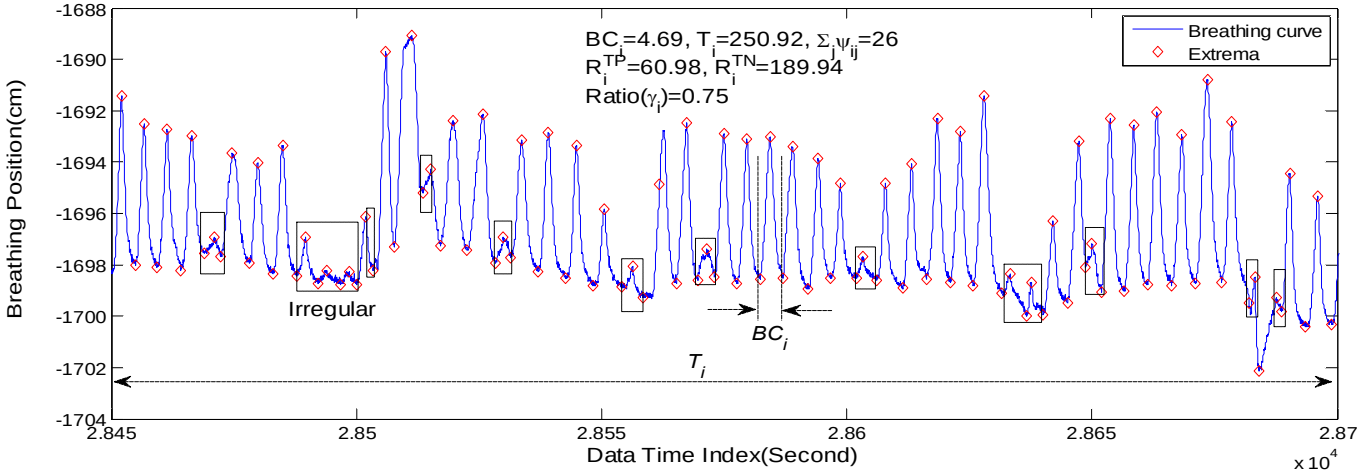


Fig. 4. True positive range ($R^{TP}$) vs. True negative range ($R^{TN}$). This figure shows how to decide $R^{TP}$ or $R^{TN}$ of patient *i* (DB17). In this example, the breathing cycle ($BC_i$), the period of observation ($T_i$), and the sum of $\psi_i$ ($\Sigma_j \psi_{ij}$) are given by the numbers of 4.69, 250.92, and 26, respectively. Accordingly, we can calculate the ratio ($\gamma_i$) of the true negative range ($R_i^{TN}$) to the period of observation ($T_i$), *i.e.*. 0.75. That means 75% of the breathing patterns during the observation period show regular breathing patterns in the given sample.

## IV. Experimental Results

### A. Breathing Motion Data

Table II shows the characteristics of the breathing datasets. The minimum and the maximum recording times are 18 and 166 minutes, respectively.

TABLE II
CHARACTERISTICS OF THE BREATHING DATASETS

| Total Patients | Average Records | Minimum Records | Maximum Records |
|---|---|---|---|
| 448 | 80 minutes | 18 minutes | 166 minutes |

To extract the feature extraction metrics in Table I, therefore, we randomly selected 18 minute samples from the whole recording time for each breathing dataset because the minimum breathing recording time is 18 minutes. That means we use 28,080 samples to get the feature extraction metrics for each breathing dataset. Every dataset for each patient is analyzed to predict the irregular breathing patterns. That means we inspect all the datasets to detect the irregular pattern ($\psi_i$) within the entire recording time. The detected irregular patterns can be used to calculate the true positive/negative ranges ($R_i^{TP}/R_i^{TN}$) and the ratio ($\gamma_i$) for the patients.

### B. Selection of the Estimated Feature Metrics ($\check{x}$)

The objective of this section is to find out the estimated feature metrics ($\check{x}$) from the candidate feature combination vector ($\bar{x}$) using discriminant criteria based on clustered degree. Fig. 5 shows all the results of the objective function (*J*) with respect to the feature metrics number. That means each column in Fig. 5 represents the number of feature extraction metrics in Table I.

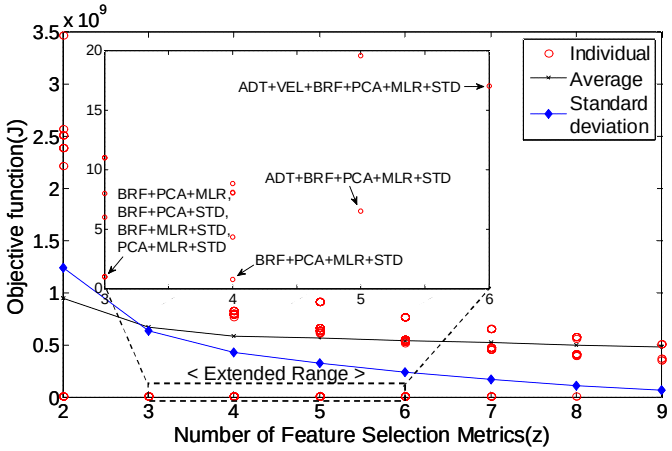


Fig. 5. Objective functions with respect to the feature metrics number to select the estimated feature metrics ($\check{x}$).

The red spot shows the objective function J(·) for each feature combination vector, whereas the black and the blue spots represent the averaged objective function and the standard deviation of the objective function with respect to the feature metrics number. We notice that two feature combination vector can have a minimal feature combination vector. Even though z=9 has the minimum standard deviation, a minimum objective function (*J*) of z=9 is much bigger than those in z=3, 4, 5 and 6 shown in Fig 5. The interesting result is that the combinations of BRF, PCA, MLR, and STD have minimum objective functions in z=3 and 4. Therefore, we would like to use these four feature extraction metrics, *i.e.*, BRF, PCA, MLR, and STD as the estimated feature vector ($\check{x}$) for the rest of modules for breathing patterns classification.

### C. Clustering of Respiratory Patterns based on EM

In this section, the breathing patterns will be arranged into groups with the estimated feature vector ($\check{x}$) for the analysis of breathing patterns.

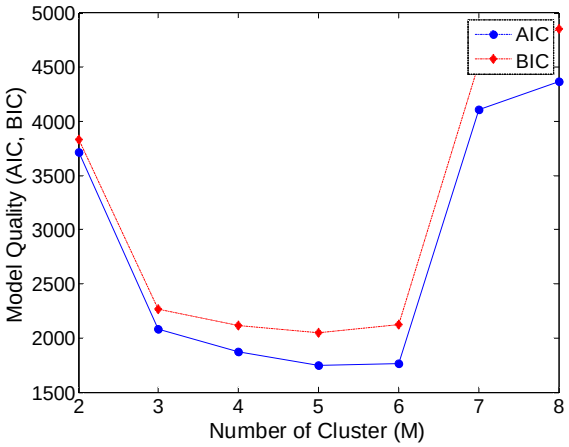


Fig. 6. Quantitative model analysis for the selection of cluster number.

In Fig. 6, we can notice that both criteria have selected the identical clustering number; M=5. Therefore, we can arrange the whole pattern datasets into five different clusters of breathing patterns based on the simulation results.

### *D. Breathing Pattern Analysis to Detect Irregular Pattern*

Before predicting irregular breathing, we analyze the breathing pattern to extract the ratio ($\gamma_i$) with the true positive and true negative ranges for each patient. For the breathing cycle ($BC_i$) we search the breathing curves to detect the local maxima and minima. After detecting the first extrema, we set up the searching range for the next extrema as 3~3.5 seconds [14]. Accordingly, we can detect the next extrema within half a breathing cycle because one breathing cycle is around 4 seconds [37]. The $BC_i$ is the mean value of the consecutive maxima or minima. Fig. 7 shows the frequency distribution of $BC_i$ for the breathing datasets. The breathing cycles are distributed with a minimum of 2.9 seconds/cycle and a maximum of 5.94 seconds/cycle. The average breathing cycle of the breathing datasets is 3.91 seconds/cycle.

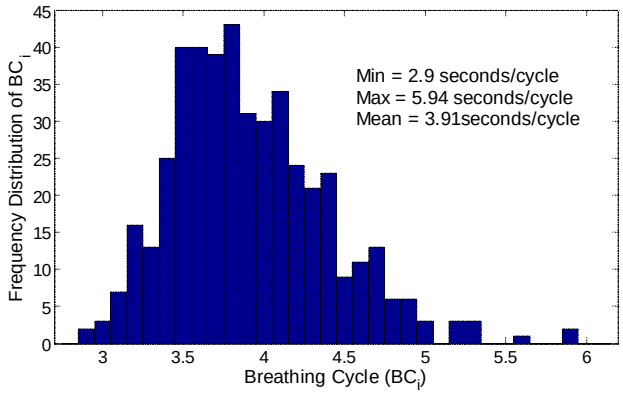


Fig. 7. Frequency distribution of breathing cycle ($BC_i$) for the breathing datasets. The breathing cycles are variable from 2.9 seconds/cycle to 5.94 seconds/cycle, with 3.91 seconds/cycle as the average time.

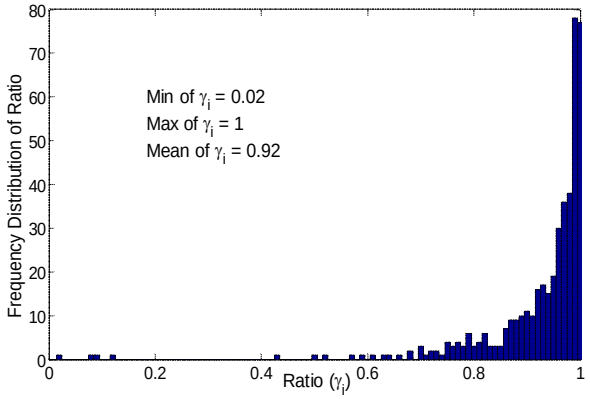


Fig. 8. Frequency distribution of ratio ($\gamma_i$). Here $\gamma_i$ is the ratio of the true negative range ($R_i^{TN}$) to the period of observation ($T_i$), thus it is dimensionless. The ratio ($\gamma_i$) for each breathing dataset is distributed from 0.02 to 1 with 0.92 as the average ratio value.

Fig. 8 shows the frequency distribution of the ratio ($\gamma_i$). Here $\gamma_i$ is the ratio of the true negative range ($R_i^{TN}$) to the period of observation ($T_i$), thus it is dimensionless. The ratio ($\gamma_i$) for each breathing dataset is distributed from 0.02 to 1 with 0.92 as the average ratio value. In Fig. 8 we can see that the frequency number of the regular breathing patterns is much higher than that of the irregular breathing patterns in the given datasets. But we can also see that it is not a simple binary classification to decide which breathing patterns are regular or irregular because the frequency distribution of the ratio is analog. We define the vague breathing patterns with the ratio 0.8~0.87 as the gray-level breathing pattern. We have shown the regular/irregular gray-level breathing patterns among the entire dataset in the following figures.

Fig. 9 shows regular breathing patterns in the given datasets. There exist several irregular points depicted with green spots. But most of breathing cycles have the regular patterns of breathing curve. Note that the regular breathing patterns have a higher ratio ($\gamma_i$) in comparison to the irregular breathing patterns.

Fig. 10 shows gray-level breathing patterns in the given datasets. Even though the gray-level breathing patterns show some consecutive irregular points, the overall breathing patterns are almost identical as shown in Fig. 10. Fig. 11 shows irregular breathing patterns in the given datasets. Note that the breathing pattern in Fig. 11(b) with a very low ratio ($\gamma_{317}$=0.51) is void of regular patterns and that there exists a mass of irregular breathing points in Fig. 11.

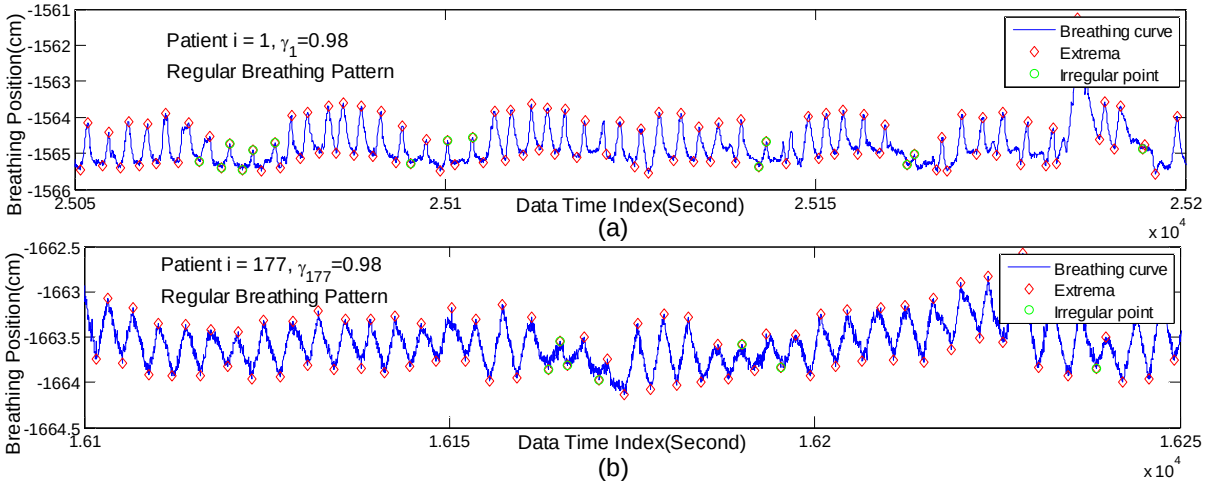


Fig. 9. Representing regular breathing patterns; (a) patient number 1 with the ratio $\gamma_1$=0.98; and (b) patient number 177 with the ratio $\gamma_{177}$=0.98.

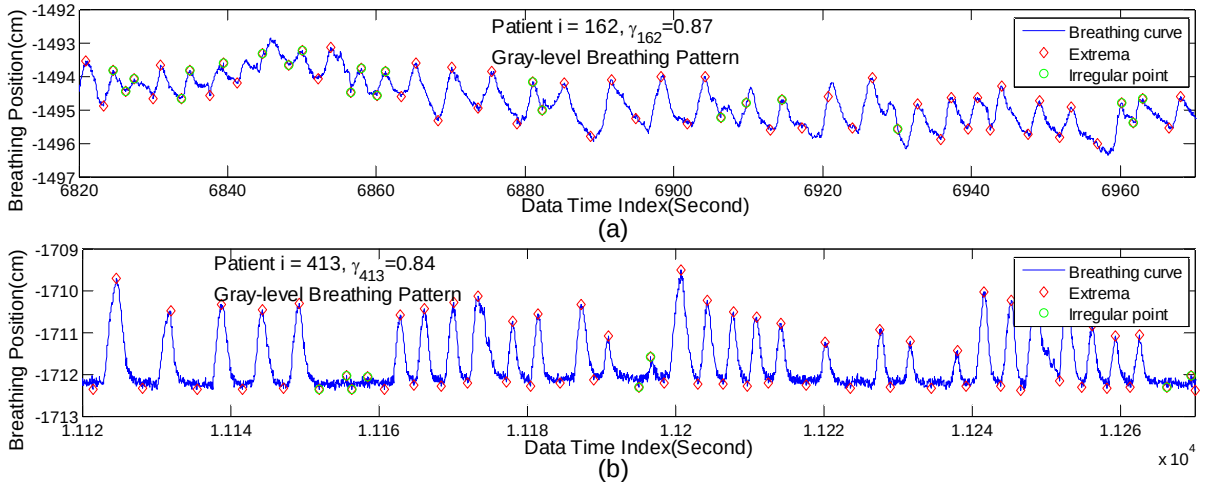


Fig. 10. Representing gray-level breathing patterns; (a) patient number 162 with the ratio $\gamma_{162}$=0.87; and (b) patient number 413 with the ratio $\gamma_{413}$=0.84.

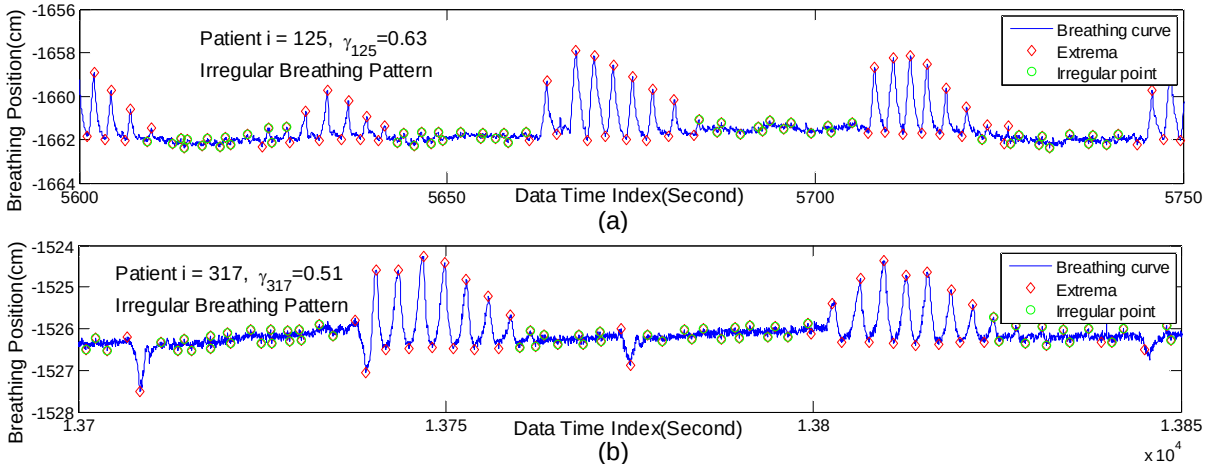


Fig. 11. Representing irregular breathing patterns; (a) patient number 125 with the ratio $\gamma_{125}$=0.63; and (b) patient number 317 with the ratio $\gamma_{317}$=0.51.

### *E. Classifier Performance*

An ROC curve is used to evaluate irregular breathing patterns with true positive rates vs. regular breathing patterns with false positive rates. For the concrete analysis of the given breathing datasets, we would like to show an ROC curve with respect to different regular thresholds. In addition, we will change the discrimination threshold by the period of observation ($T_i$) to validate the performance of the proposed binary classifier system. To predict the irregular breathing patterns from the patient datasets, we may evaluate the classification performance by showing the following two ROC analyses:

In the first ROC, we may increase the threshold value $\xi_m$ defined in (16) in Section III.D from 0.1 to 0.99. By changing

the observation period $T_i$ to 900, 300, and 100 seconds, the system may include the irregular breathing patterns extracted under the different parameters of $\xi_m$. Specifically, depending on the observation period $T_i$, we would like to adjust the threshold value $\xi_m$ for the ROC evaluation of the proposed classifier.

In the second ROC, we may increase the regular threshold ($\Psi_{th}$) so that the patient datasets with the ratio ($\gamma_i$) of patient $i$ may be changed from true negative to true positive. For the analysis based on the regular threshold, we extract the ratio ($\gamma_i$) of patient $i$ by changing the observation period $T_i$ of 900, 300, and 100 seconds. The regular threshold $\Psi_{th}$ can be variable from 0.1 to 0.99, especially by changing the regular threshold $\Psi_{th}$ of 0.80, 0.85, and 0.90, defined in Section IV.A. Depending on the regular threshold ($\Psi_{th}$), ROC is analyzed for the performance of the proposed classifier.

After we make a class for each breathing pattern, and analyze breathing patterns to detect irregular patterns, the free parameters of neural networks are determined by the 28,080 training samples of multiple patient datasets for each class, where these samples are used as input with 10 iterations through the process of providing the network and updating the networkôs free parameters. We evaluate the classification performance whether the breathing patterns are irregular or regular to extract the true positive/negative ranges and the ratio as shown in Fig. 12. To decide the regular/irregular breathing pattern of the patient datasets, we have varied observation periods ($T_i$) for feature extraction with 900, 300, and 100 seconds. Fig. 12 shows ROC graphs to evaluate how different observation periods affect the classification performance. Here, we fixed the regular threshold $\Psi_{th}$ of 0.92 that is the mean value of the ratio ($\gamma_i$).

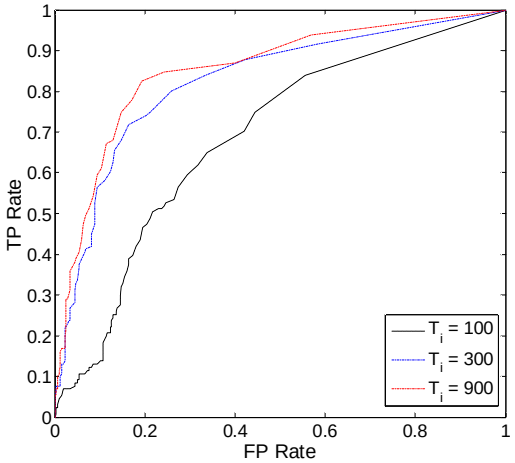


Fig. 12. ROC graph of irregular detection with different observation period.

In Fig. 12, we can see that the proposed classifier shows a better performance with a long observation period ($T_i$). The more observation periods we have, the better performance we obtain in the proposed classifier. That means the classifier can be improved by extending the observation period for feature extraction.

Fig. 13 shows ROC graphs of irregular detection with different regular thresholds $\Psi_{th}$ of 0.8, 0.85, and 0.9. In this figure, the ratio ($\gamma_i$) of patients $i$ are extracted with observation periods $T_i$ of 100, 300, and 900 seconds.

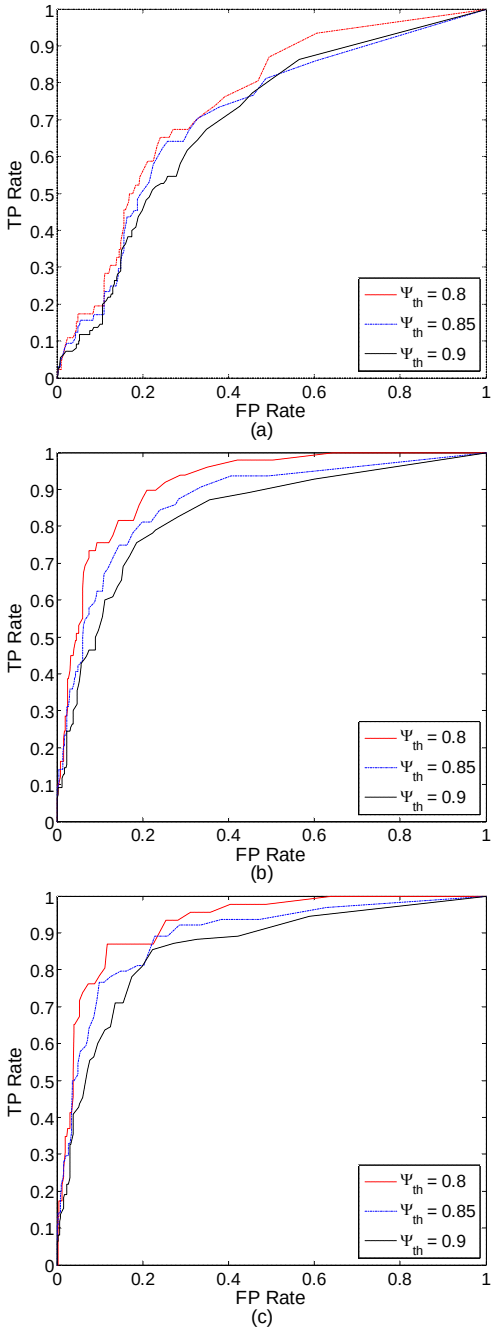


Fig. 13. ROC graph of irregular detection with different regular thresholds and observation period; (a) observation period $T_i$ = 100 seconds, (b) observation period $T_i$ = 300 seconds, and (c) observation period $T_i$ = 900 seconds.

The different regular thresholds $\Psi_{th}$ also affect the classifier performance. The classifier performance is slightly improved by lowering the regular thresholds. The smaller the regular threshold $\Psi_{th}$, the better the classifier performance. Here, we notice that the true positive rate for the proposed classifier is 97.83% when the false positive rate is 50% in Fig. 13(c).

Based on the result of ROC graph in Fig. 13 (c), we notice that the breathing cycles of any given patient with a length of at least 900 seconds can be classified reliably enough to adjust the

safety margin prior to therapy in the proposed classification. For the overall analysis of the curve, we have shown the area under the ROC curve (AUC) in Fig. 14. The AUC value can be increased by lowering the regular threshold $\Psi_{th}$. The maximum AUCs for observation period $T_i$ of 100, 300, and 900 seconds are 0.77, 0.92, and 0.93, respectively. Based on Fig. 14, Fig. 13 (a)-(c) picked 0.8, 0.85, and 0.9 for $\Psi_{th}$.

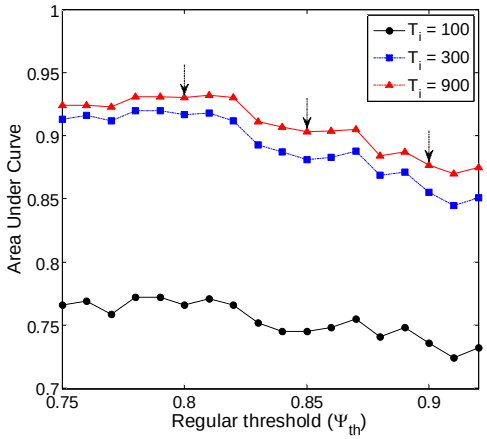


Fig. 14. Area under the ROC curve. The maximum AUCs for the observation period $T_i$ of 100, 300, and 900 seconds are 0.77, 0.92, and 0.93, respectively.

We show the computational efficiency of the proposed method with CPU time used to train the proposed classifier with the given sample sets and to classify the patient datasets for its applicability to practical scenarios. The following table shows the CPU time used for the training and classification time of the proposed algorithm for each class.

TABLE III
CPU TIME USED FOR THE COMPUTATIONAL EFFICIENCY

| Class (Patient number) | Class 1 (123) | Class 2 (23) | Class 3 (64) | Class 4 (107) | Class 5 (131) |
|---|---|---|---|---|---|
| CPU Time used (sec.) | 46.609 | 1.046 | 9.546 | 38.296 | 67.531 |

As shown in Table III, the CPU time used can be increased with regard to the number of patients. The average computational time for each class is 289 ms per patient.

Some studies investigated the classification of regular/irregular breathing patterns for the detection of lung diseases with spirometry [8-11]. Irregular breathing patterns can also impact on the dosimetric treatment for lung tumors in stereotactic body radiotherapy [6, 12-13]. However, there are few studies with the results on the classification of breathing irregularity in this area. The following table shows the classification performance of irregular breathing detection using a variety of respiratory measurement datasets.

TABLE IV
CLASSIFIER STUDIES OF IRREGULAR BREATHING DETECTION

| Studies | Performance | Measurement Datasets | Methods |
|---|---|---|---|
| Regular/Irregular classification [9] | TPR: 92.6% | Spirometry data of 250 | ANN-based |
| Regular/Irregular classification [10] | TPR: 97.5% | Spirometry data of 205 | ANN-based |
| Regular/Irregular classification [11] | TP/(TP+FP): 98% | 74 sleep disordered breathing data | ANN-based |
| **Proposed classification** | **TPR: 97.8%** | **Breathing motion data of 448** | **EM/ANN -based** |

TPR: True Positive Rate, ANN: Artificial Neural Network

Table IV shows the classification performances of the irregular detection with other methods and measurement datasets. The existing classifier studies demonstrated that spirometry data using an ANN-based approach could provide a good performance of breathing classification, *i.e.* TPR 92.6% [9] and 97.5% [10]. Our proposed method can also provide similar or better performance (TPR 97.8%) of breathing classification with an EM/ANN-based approach. Please note that the classification performance of the proposed method is based on breathing motion datasets of more than 400 patients. Sleep-disorder data showed a better performance of 98% TP(TP+FP) [11]. However, sleep-disorder data are not applicable for breathing motion assessment of lung cancer treatment in patients with usually compromised lung function; in addition, the breathing dataset was limited to sleep-disordered breathing data of 74 patients. Our proposed classification shows results of the classifier performance of 97.83% TPR with 448 samples breathing motion data. That means the proposed classifier can achieve acceptable results comparable to the classifier studies using the spirometry data.

The proposed method assumes that the data used to build the classifier is representative enough of breathing patterns of other subjects in general. It also assumes that the breathing pattern of a human captured at some point in time before the treatment is indicative of its future breathing patterns. The proposed system with this value is not intended to be used as real time classification system.

The proposed methodology is based on the three-coordinate breathing datasets for external beam radiation treatment. Typically, radiation treatment is delivered after a planning process in which x-ray imaging and advanced treatment planning are prepared. Spirometry is not used for radiotherapy planning or delivery except for breath hold treatment to which motion prediction does not apply. Reasons for not using spirometry might be that it does not provide any directional data and that it might be not tolerable in all lung cancer patients to continuously monitor respiration due to compromised lung function. The proposed method with breathing datasets may provide clinical advantages to adjust the dose rate before and during the external beam radiotherapy for minimizing the safety margin.

## V. CONCLUSIONS

In this paper we have presented an irregular breathing classifier that is based on the regular ratio (γ) detected in multiple patients-datasets. Our new method has two main contributions to classify irregular breathing patterns. The first contribution is to propose a new approach to detect abnormal breathing patterns with multiple patientsô breathing data that better reflect tumor motion in a way needed for radiotherapy than spirometry data. The second contribution is that the proposed new method achieves the best irregular classification performance by adopting EM based on the Gaussian Mixture model with the usable feature combination from the given feature extraction metrics.

The proposed irregular breathing classification used a regular ratio to decide whether or not the current breathing

patterns are regular. The particular ratio value may be used to individually adjust the margin size for radiation treatment delivery. The patients classified with regular breathing patterns would be treated with tight margins to minimize projection span and thereby allow better normal tissue sparing. The patients classified with irregular breathing patterns may have their safety margins adjusted based on the irregular patterns to cope with baseline shifts or highly fluctuating amplitudes that are not covered by population-based safety margins.

The recorded breathing motions of 448 patients include regular and irregular patterns in our testbed. With the proposed method, the breathing patterns can be divided into regular/irregular breathing patterns based on the regular ratio ($\gamma$) of the true negative range to the period of observation. The experimental results validated that our proposed irregular breathing classifier can successfully detect irregular breathing patterns based on the ratio, and that the breathing cycles of any given patient with a minimum length of 900 seconds can be classified reliably enough to adjust the safety margin prior to therapy in the proposed classification.

## ACKNOWLEDGMENTS

This study was supported in part by the deanôs office of the School of Engineering at Virginia Commonwealth University, and NSF ECCS #1054333. The work reported here would not be possible without the help of M. Murphy and J. Williamson.

## REFERENCES

[1] P. J. Keall, G. S. Mageras, J. M. Balter, R. S. Emery, K. M. Forster, S. B. Jiang, J. M. Kapatoes, D. A. Low, M. J. Murphy, B. R. Murray, C. R. Ramsey, M. B. Van Herk, S. S. Vedam, J. W. Wong, and E. Yorke, ñ*The management of respiratory motion in radiation oncology report of AAPM Task Group 76*,ò *Med. Phys.*, vol. 33, no. 10, pp 3874-3900, 2006.

[2] H. Murshed , H. H. Liu , Z. Liao, J. L. Barker, X. Wang, S. L. Tucker, A. Chandra, T. Guerrero, C. Stevens, J. Y. Chang, M. Jeter, J. D. Cox, R. Komaki and R. Mohan, ñDose and volume reduction for normal lung using intensity-modulated radiotherapy for advanced-stage non-small-cell lung cancer,ò *Int. J. Radiat. Oncol. Biol. Phys.*, vol. 58, no. 4, pp. 1258-1267, 2004.

[3] P. S. Verma, H. Wu, M. P. Langer, I. J. Das and G. Sandison, ñReview of real-time tumor motion prediction for Image Guided Radiation Treatment,ò *Computing in Science & Engineering*, no. 99, 2010.

[4] M. J. Murphy and S. Dieterich, ñ*Comparative performance of linear and nonlinear neural networks to predict irregular breathing*,ò *Phys. Med. Biol.*, no. 51, pp, 5903ï 5914, 2006.

[5] K. Malinowski, T. J. McAvoy, R. George, S. Dietrich and W. D. DôSouza, ñ*Incidence of Changes in Respiration-Induced Tumor Motion and Its Relationship with Respiratory Surrogates during Individual Treatment Fractions*,ò *Int J Radiat Oncol Biol Phys.*, pp 1-9, 2011.

[6] I. Buzurovic, K. Huang, Y. Yu and T. K. Podder, ñ*A robotic approach to 4D real-time tumor tracking for radiotherapy*,ò *Phys. Med. Biol.*, no. 56, pp 1299ï 1318, 2011.

[7] A. Lanatà, E. P. Scilingo, E. Nardini, G. Loriga, R. Paradiso and D. De-Rossi, ñ*Comparative Evaluation of Susceptibility to Motion Artifact in Different Wearable Systems for Monitoring Respiratory Rate*,ò *IEEE Trans. Inf. Technol. Biomed.*, vol. 14, no. 2, pp. 378-386, 2010.

[8] A. Cohen and D. Landsberg, ñ*Analysis and Automatic Classification of Breath Sounds*,ò *IEEE Trans. Biomed. Eng.*, vol. 31, no. 9, 1984.

[9] M. J. Baemani, A. Monadjemi, and P. Moallem, ñ*Detection of Respiratory Abnormalities Using Artificial Neural Networks*,ò *J Computer Science*, vol. 4, no. 8, pp. 663-667, 2008.

[10] S. Jafari, H. Arabalibeik and K. Agin, ñ*Classification of normal and abnormal respiration patterns using flow volume curve and neural network*,ò *International Symposium on Health Informatics and Bioinformatics*, pp. 110-113, 2010.

[11] I. Ayappa, R. G. Norman, D. Whiting, A. H. W. Tsai, F. Anderson, E. Donnely, D. J. Silberstein, and D. M. Rapoport, ñ*Irregular Respiration as a Marker of Wakefulness during Titration of CPAP*,ò *Sleep*, vol. 32, no. 1, pp. 99 - 104, 2009.

[12] L. Huang, K. Park, T. Boike, P. Lee, L. Papiez, T. Solberg, C. Ding and R. D. Timmerman, ñ*A study on the dosimetric accuracy of treatment planning for stereotactic body radiation therapy of lung cancer using average and maximum intensity projection images*,ò *Radiotherapy and Oncology*, vol. 96, no. 1, pp. 48 - 54, 2010

[13] Y. D. Mutaf, C. J. Scicutella, D. Michalski, K. Fallon, E. D. Brandner, G. Bednarz and M. S. Huq, ñ*A simulation study of irregular respiratory motion and its dosimetric impact on lung tumors*,ò *Phys. Med. Biol.*, vol. 56, no. 3, pp. 845 - 859, 2011.

[14] G. Benchetrit, ñ*Breathing pattern in humans: diversity and individuality*,ò *Respiration Physiology*, no. 122, pp. 123ï 129, 2000.

[15] P. Chazal, M. OôDwyer, and R. B. Reilly, ñ*Automatic Classification of Heartbeats Using ECG Morphology and Heartbeat Interval Features*,ò *IEEE Trans. Biomed. Eng.*, vol. 51, no. 7, pp. 1196-1206, 2004.

[16] P. Chazal, and R. B. Reilly, ñ*A Patient-Adapting Heartbeat Classifier Using ECG Morphology and Heartbeat Interval Features*,ò *IEEE Trans. Biomed. Eng.*, vol. 53, no. 12, pp. 2535-2543, 2006.

[17] M. Hoogeman, JB Prévost, J. Nuyttens, J. Pöll, P. Levendag P, B. Heijmen, ñ*Clinical accuracy of the respiratory tumor tracking system of the cyberknife: assessment by analysis of log files*,ò *Int J Radiat Oncol Biol Phys.*, vol. 74, no. 1, pp. 297-303, 2009.

[18] A. P. King, K. S. Rhode, R. S. Razavi, and T. R. Schaeffter, ñ*An Adaptive and Predictive Respiratory Motion Model for Image-Guided Interventions: Theory and First Clinical Application*,ò *IEEE Trans. Med. Imag.*, vol. 28, no. 12, pp. 2020 - 2032, 2009.

[19] J. Ehrhardt, R. Werner, A. Schmidt-Richberg, and H. Handels, ñ*Statistical Modeling of 4D Respiratory Lung Motion Using Diffeomorphic Image Registration*,ò *IEEE Trans. Med. Imag.*, vol. 30, no. 2, pp. 251 - 265, 2011.

[20] W. Bai and S. M. Brady, ñ*Motion Correction and Attenuation Correction for Respiratory Gated PET Images*,ò *IEEE Trans. Med. Imag.*, vol. 30, no. 2, pp. 351 - 365, 2011.

[21] S. J. Lee, Y. Motai, and M. Murphy, ñ*Respiratory Motion Estimation with Hybrid Implementation of Extended Kalman Filter*,ò *IEEE Trans. Ind. Electron.*, In Press, 2011.

[22] F. Pernkopf and D. Bouchaffra, ñ*Genetic-based EM algorithm for learning Gaussian mixture models*,ò *IEEE Trans. Pattern Analysis and Machine Intelligence*,ò vol. 27, no. 8, pp. 1344 ï 1348, 2005.

[23] V. Chandola, A. Banerjee, and V. Kumar, ñ*Anomaly Detection: A Survey*,ò *ACM Computing Surveys*, vol. 41, no. 3, 2009.

[24] M. A. Kupinski, D. C. Edwards, M. L. Giger, and C. E. Metz, ñ*Ideal Observer Approximation Using Bayesian Classification Neural Networks*,ò *IEEE Trans. Med. Imag.*, vol. 20, no. 9, pp 886-899, 2001.

[25] M. J. Murphy and D. Pokhrel, ñ*Optimization of an adaptive neural network to predict breathing*,ò *Med. Phys.*, vol. 36, no. 1, pp. 40-47, 2009.

[26] P. Guo, C.L. P. and M. R. Lyu, ñ*Cluster number selection for a small set of samples using the Bayesian Ying-Yang model*,ò *IEEE Trans. Neural Netw.*, vol. 13, no. 3, pp. 757-763, 2002.

[27] S. Haykin, *Neural Networks and Learning Machines*. 3rd edn, Pearson, 2009.

[28] R. O. Duda, P. E. Hart and D. G. Stork, *Pattern Classification*. John Wiley & Sons, 2001.

[29] Z. Li, D. Lin and X. Tang, ñ*Nonparametric Discriminant Analysis for Face Recognition*,ò *IEEE Trans. Pattern Analysis and Machine Intelligence*, vol. 31, no. 4, 2009.

[30] T. Fawcett, ñ*An introduction to ROC analysis*,ò *Pattern Recognition Letters*, vol. 27, no. 8, 2006.

[31] K. P. Burnham and D. R. Anderson, *Model selection and multi-model inference: a practical information-theoretic approach*. New York: Springer-Verlag, 2002.

[32] C. I. Christodoulou, C. S. Pattichis, M. Pantziaris and A. Nicolaides, ñ*Texture-Based Classification of Atherosclerotic Carotid Plaques*,ò *IEEE Trans. Med. Imag.*, vol. 22, no. 7, 2003.

[33] W. Chen, C. E. Metz, M. L. Giger, and K. Drukker, ñ*A Novel Hybrid Linear/Nonlinear Classifier for Two-Class Classification: Theory, Algorithm, and Applications*,ò *IEEE Trans. Med. Imag.*, vol. 29, no. 2, pp 428-441, 2010.

[34] T. Mu, T. C. Pataky, A. H. Findlow, M. S. H. Aung and J. Y. Goulermas, ñ*Automated Nonlinear Feature Generation and Classification of Foot Pressure Lesions*,ò *IEEE Trans. Inf. Technol. Biomed.*, vol. 14, no. 2, pp. 418-424, 2010.

[35] H. Atoui, J. Fayn and P. Rubel, ñ*A Novel Neural-Network Model for Deriving Standard 12-Lead ECGs From Serial Three-Lead ECGs: Application to Self-Care*,ò *IEEE Trans. Inf. Technol. Biomed.*, vol. 14, no. 3, pp. 883-890, 2010.

[36] S. S. Vedam, P. J. Keall, A. Docef, D. A. Todor, V. R. Kini and R. Mohan, ñ*Predicting respiratory motion for four-dimensional radiotherapy*,ò *Med. Phys.*, vol. 31, no. 8, pp. 2274 -2283, 2004.

[37] W. Lu, M. M. Nystrom, P. J. Parikh, D. R. Fooshee, J. P. Hubenschmidt, J. D. Bradley, and D. A. Low, ñ*A semi-automatic method for peak and valley detection in free-breathing respiratory waveforms*,ò *Med. Phys.*, vol. 33, no. 10, pp. 3634 -3636, 2006.

[38] V. Srinivasan, C. Eswaran, and N. Sriraam, ñ*Approximate Entropy-Based Epileptic EEG Detection Using Artificial Neural Networks*,ò *IEEE Trans. Inf. Technol. Biomed.*, vol. 11, no. 3, pp. 288-295, 2007.

[39] R. Berbeco, S. Nishioka, H. Shirato, G. Chen and S. B. Jiang, ñ*Residual motion of lung tumours in gated radiotherapy with external respiratory surrogates*,ò *Phys. Med. Biol.*, vol. 50, no. 16, pp. 3655-3667, 2005.

[40] A. H. Khandoker, J. Gubbi and M. Palaniswami, ñ*Automated Scoring of Obstructive Sleep Apnea and Hypopnea Events Using Short-Term Electrocardiogram Recordings*,ò *IEEE Trans. Inf. Technol. Biomed.*, vol. 13, no. 6, pp. 1057-1067, 2009.

[41] J. Zhao and P. L. H. Yu, ñFast ML Estimation for the Mixture of Factor Analyzers via an ECM Algorithm,ò *IEEE Trans. Neural Netw.*, vol. 19, no. 11, pp. 1956-1961, 2008.

Suk Jin Lee (Sôî1) received the B.Eng. degree in electronic engineering and the M.Eng. degree in telematics engineering from Pukyong National University, Busan, Korea, in 2003 and 2005, respectively, and the Ph.D. degree in electrical and computer engineering from Virginia Commonwealth University, Richmond, VA, in 2012. In 2007 he worked as a visiting research scientist at GW Center for Networks Research, George Washington University. His research interests include network protocols, neural network, target estimate, and classification.

Yuichi Motai (Mô01) received the B.Eng. degree in instrumentation engineering from Keio University, Tokyo, Japan, in 1991, the M.Eng. degree in applied systems science from Kyoto University, Kyoto, Japan, in 1993, and the Ph.D. degree in electrical and computer engineering from Purdue University, West Lafayette, IN, U.S.A., in 2002. He is currently an Assistant Professor of Electrical and Computer Engineering at Virginia Commonwealth University, Richmond, VA, USA. His research interests include the broad area of sensory intelligence; particularly in medical imaging, pattern recognition, computer vision, and sensory-based robotics.

Elisabeth Weiss graduated from the University of Würzburg, Germany in 1990 and received her doctorate degree in 1991. After participating in various residency programs in Berne (Switzerland), Würzburg (Germany), and Tübingen (Germany), she completed her residency in radiation oncology at the University of Göttingen (Germany) in 1997, and received an academic teacherôs degree in 2004. She is currently a professor in the Department of Radiation Oncology. At VCU, she works as a research physician with the Medical Physics Division and participates in the development of image-guided radiotherapy techniques and 4D radiotherapy of lung cancer.

Shumei S. Sun received a B.P.H (Public Health) degree from the College of Medicine at National Taiwan University, Taiwan in 1976, the M.S. degree in applied mathematics and statistics from the State University of New York, NY, USA in 1980, and the Ph.D. degree in biostatistics from the University of

Pittsburgh, PA, USA in 1983. She is currently a department chair and professor with the Department of Biostatistics, School of Medicine, Virginia Commonwealth University, Richmond. Her research interests include the broad area of understanding the natural history of human growth, body composition, and risk factors for cardiovascular and related diseases in the human lifespan, and to indirectly improve the quality of life through health promotion and disease prevention.